Processing and Mechanical Properties of Directionally Solidified NiAl/NiAlTa Alloys

D. R. Johnson, B. F. Oliver
The University of Tennessee, Knoxville, TN 37996-2200

R. D. Noebe, and J. D. Whittenberger
NASA-Lewis Research Center, Cleveland, OH 44135

ABSTRACT

Promising creep strengths were found for a directionally solidified NiAl-NiAlTa alloy when compared to other NiAl based intermetallics. The directionally solidified alloy had an off-eutectic composition that resulted in microstructures consisting of NiAl dendrites surrounded by aligned eutectic regions. The room temperature toughness of the two phase alloy was similar to that of polycrystalline NiAl even with the presence of the brittle Laves phase NiAlTa. Alloying additions that may improve the room temperature toughness by producing multiphase alloys are discussed.

INTRODUCTION

The intermetallic compound NiAl is a potential material for use at elevated temperatures, due to its superior oxidation resistance, high melting point, and high thermal conductivity [1]. However, NiAl is brittle at room temperature and has poor elevated temperature strength, both of which render this material inadequate for structural applications. Reinforcing NiAl with second phases to form composite materials may eliminate these problems.

One method for producing NiAl-based composites is by controlling the eutectic solidification process of NiAl based alloys. During eutectic growth, two or more solid phases form simultaneously from the liquid. Directional solidification of these eutectic alloys may produce in-situ composites, where one or more phases are aligned parallel to the growth direction.

Sauthoff has shown that Laves phases such as NiAlNb and NiAlTa can be used to strengthen NiAl [2,3]. In general, the improvement in strength increases with the greater volume fraction of Laves phase present. However, eutectic microstructures are possible within these systems allowing

Processing and Fabrication of Advanced Materials III
Edited by V.A. Ravi, T.S. Srivatsan and J.J. Moore
The Minerals, Metals & Materials Society, 1994

for in-situ composite studies. For example, Whittenberger et. al. have found that the creep strength of the NiAl-NiAlNb eutectic is extremely sensitive to microstructure and processing conditions [4]. By directional solidification of this eutectic, an order of magnitude increase in creep resistance was measured when compared to materials processed using a casting and extrusion procedure. Unfortunately, the creep strength of the NiAl-NiAlNb alloys is still less than that of the Ni-base superalloys.

While the phase equilibria of the NiAl-NiAlTa system are not as well known [5], alloys from this system may display better strengths than the NiAl-NiAlNb alloys. The recent developments of in-situ composites based on NiAl-NiAlTa alloys are discussed in this paper. Preliminary results from alloying studies, processing, and mechanical testing are discussed.

EXPERIMENTAL

As a first approach to locating promising microstructures for in-situ composite studies, alloys containing high purity Ni, Al, and Ta were arc-melted with a non-consumable tungsten electrode into approximately 12 gram buttons. To promote homogeneity, each button was melted at least five times and flipped between each melting. Arc-melted ingots were metallographically prepared and etched with a solution of 5%HF-5%HNO_3-90%H_2O.

From the survey study, selectively chosen alloys were then cast into 25.4 mm diameter, 1 Kg ingots and directionally solidified at 20 mm/h to produce near equilibrium microstructures. Directional solidification was performed in the containerless mode by the electromagnetically-levitated zone process [6,7]. The processed sections of these ingots were approximately 25 mm in diameter and 75 mm in length.

Elevated temperature properties of the NiAl-NiAlTa alloys were determined by compression tests at 1200, 1300 and 1400 K. Compressive properties were generated under both constant velocity conditions in a screw driven universal machine and under constant load conditions in compressive creep machines. In general, constant velocity experiments were used to determine behavior at fast strain rates ($>10^{-6}$ s^{-1}) while constant load testing was employed for lower rates. All testing was performed in air as a secondary check for environmental resistance. The cylindrical compression specimens, 5 mm diameter by 10 mm long, were machined with the length of each specimen parallel to the growth direction.

The room temperature toughness was determined by performing four-point bend tests. The specimen size and test geometry are shown in Figure 1. Bend specimens were electrical discharge machined and notched perpendicular to the growth direction using a slow speed diamond impregnated saw. A fatigue crack was not initiated at the notch tip prior to testing. Bend tests were performed on a servo-hydraulic test frame using a displacement rate of $7.6x10^{-4}$

mm/s. Fracture toughness values were calculated using the K calibration for pure bending [8].

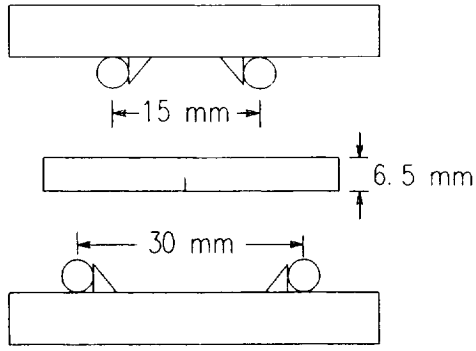

Figure 1: Geometry of four-point flexure testing fixture.

MICROSTRUCTURES

Eutectic microstructures consisting of NiAl and NiAlTa were found in arc-melted ingots containing 14 to 16 atomic percent Ta. This eutectic is characterized by a lamellar microstructure and has a melting temperature near 1820 K as determined by differential thermal analysis (DTA). From the series of arc-melted ingots, an induction melted and drop cast ingot having a composition of NiAl-14.5 Ta (at%) was directionally solidified for mechanical property testing.

The microstructure of the NiAl-14.5 Ta ingot consisted of NiAl dendrites and eutectic colonies. Since the directionally solidified ingot was processed at near equilibrium conditions, the dendritic microstructure represents an off eutectic composition. To better determine the eutectic composition, another NiAl-14.5 Ta ingot was directionally solidified with a small amount of Ta added to the initial molten zone. The added Ta produced a well aligned microstructure for the beginning section of the ingot. An eutectic composition of NiAl-15.5 Ta (at%) was determined for this region by inductively coupled plasma atomic emission spectroscopy.

The longitudinal microstructures for the arc-melted and directionally solidified alloys are shown in Figure 2. The difference in the arc-melted and directionally solidified microstructures suggests, that for rapid solidification rates, the couple growth region is skewed towards lower Ta contents at moderate undercoolings. Such high solidification rates and undercoolings are produced by the water cooled hearth during arc-melting.

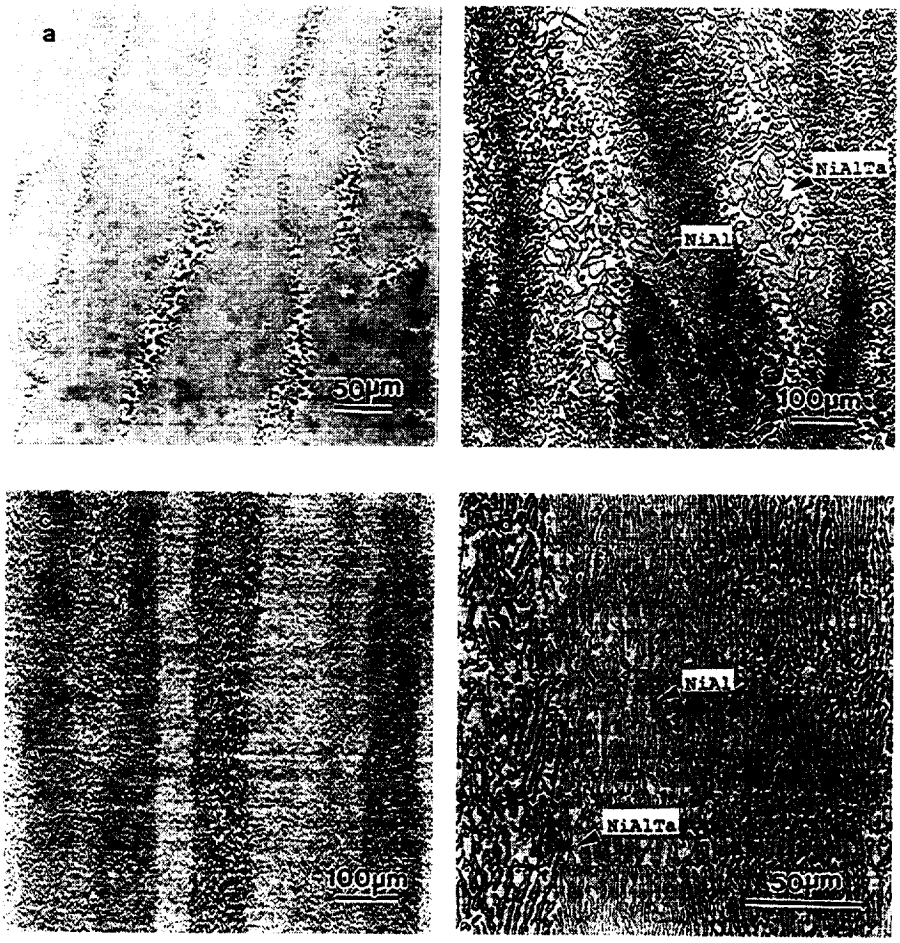

Figure 2: Light optical photomicrographs of arc-melted and directionally solidified NiAl-NiAlTa alloys.
(a) Arc-melted ingot (NiAl-14.5 Ta)
(b) Directionally solidified ingot (NiAl-14.5 Ta, 20 mm/h)
(c) Directionally solidified ingot (NiAl-15.5 Ta, 20 mm/h)
(d) Directionally solidified ingot (NiAl-15.5 Ta, 20 mm/h)

ELEVATED TEMPERATURE STRENGTH

The directionally solidified NiAl-14.5 Ta alloy has a very good compressive creep strength when compared to binary NiAl. The flow stress and strain rate data for this material were fitted to a form of the Dorn equation describing the steady-state creep rate, $\dot{\varepsilon}$, as:

$$\dot{\varepsilon} = A\sigma^{n}\exp(-Q/RT)$$

where A is a constant, σ is the applied true stress (MPa), Q is the activation energy (kJ/mol), T is the absolute temperature, R is the gas constant, and n is the stress exponent. The creep behavior for the NiAl-NiAlTa alloy can be compared to that of NiAl-NiAlNb and NiAl in Table 1.

Table 1: Representative Creep Behavior for NiAl-Laves alloys compared to binary NiAl.

Alloy	Representative creep behavior
NiAl [001] (Ni-50Al)	1100-1300 K (ref. 9): $\dot{\varepsilon} = (0.16)\sigma^{5.75}\exp(-314.2/RT)$
NiAl-NiAlNb (Ni-41.75Al-16.5Nb)	1200-1300 K (ref. 4): $\dot{\varepsilon} = (40.0)\sigma^{4.17}\exp(-414.5/RT)$
NiAl-NiAlTa (Ni-42.74Al-14.5Ta)	1200-1400 K (this work): $\dot{\varepsilon} = (4.55\text{x}10^{3})\sigma^{4.91}\exp(-521.6/RT)$

Comparing the NiAl-Laves alloys to binary NiAl reveals a decrease in the stress exponent. However, the NiAl-NiAlTa alloy has a much higher activation energy. The improved creep strength of the NiAl-NiAlTa alloy is further illustrated in Figure 3 which displays the 1300 K creep strengths of several NiAl based alloys and a Ni-based superalloy.

While the creep strength of the NiAl-NiAlTa alloy is less than that of the Ni-based superalloys, it should be noted that the microstructure of this NiAl-NiAlTa alloy is far from optimum. The microstructure of this alloy is dendritic and poorly aligned, Figure 2b. Further improvements in creep strength are expected from a fully eutectic, well-aligned microstructure.

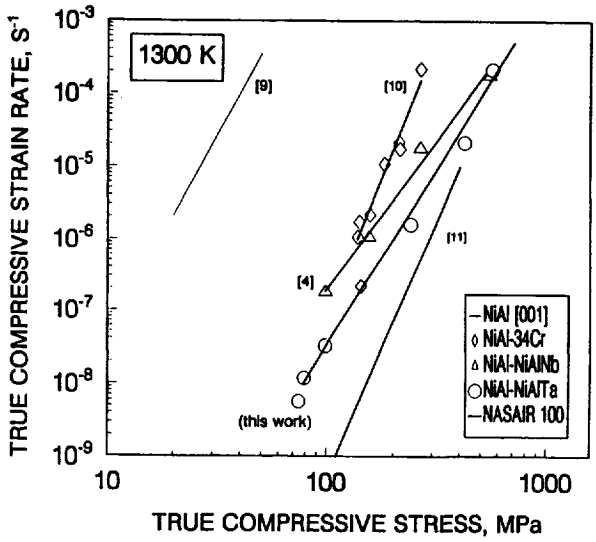

Figure 3: Compressive flow stress-strain rate behavior for several NiAl-based alloys at 1300 K.

ROOM TEMPERATURE TOUGHNESS

As expected, the NiAl-NiAlTa alloys are brittle at room temperature with a fracture toughness of approximately 5 MPa$\sqrt{m}$ as measured from nine bend specimens. Table 2 lists the fracture toughness of various NiAl-based materials for comparison.

Table 2: Room temperature fracture toughness of alloys containing NiAl, Laves phases, and refractory metal phases.

Material	morphology	Fracture toughness (MPa$\sqrt{m}$)	
NiAl	polycrystalline (HIP)	6	(ref. 12)
NiAlNb	single phase (HIP)	2	(ref. 13)
NiAl-NiAlNb	eutectic (cast)	4	(ref. 13)
NiAl-Cr	eutectic (DS)	20.6 ±1.2	(ref. 14)
NiAl-NiAlTa	near eutectic (DS)	5.1 ±0.8	(this work)

HIP = hot isostatically pressed powder metallurgy
DS = directionally solidified

From Table 2, the NiAl-NiAlTa alloy has a fracture toughness comparable to that of polycrystalline NiAl. Hence, the large increase in creep strength of the NiAl-Laves phase alloys is not gained at the expense of fracture toughness.

The fracture surface of a NiAl-NiAlTa bend specimen is shown in Figure 4. The eutectic microstructure is remarkably visible from the fracture surface as a result of partial debonding between phases during fracture. Further evidence of this fracture behavior is shown in Figure 5. A section of the directionally solidified NiAl-NiAlTa ingot was polished and then broken with the polished surface in tension. The resulting fracture profile reveals that the Laves phase fractures first with the crack bridging the NiAl phase. In addition, cracking is also visible along the NiAl/NiAlTa phase boundary. The above data suggest that the NiAl phase provides most of the fracture toughness in these brittle alloys.

One possible scheme for improving the toughness of the NiAl-NiAlTa alloys may be to increase the fracture toughness of the NiAl phase by further alloy additions. Of particular interest are systems having a metallic phase for better low temperature toughness combined with intermetallic phases for good elevated temperature strength.

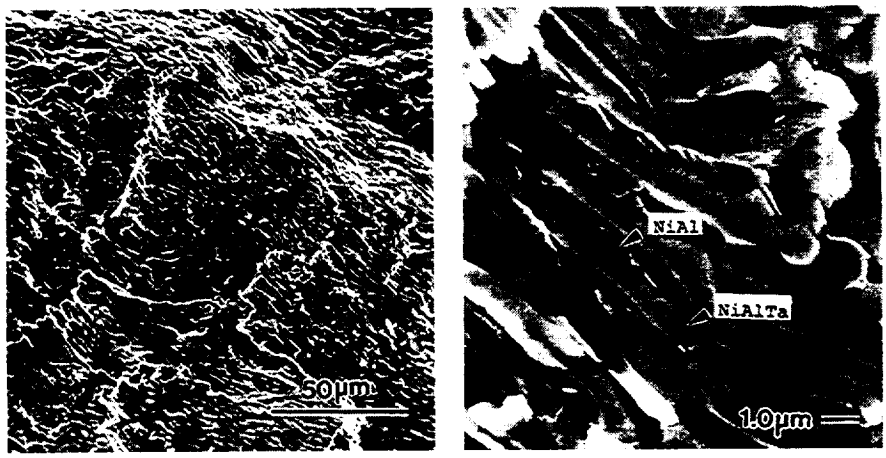

Figure 4: SEM photomicrographs of fracture surfaces from a NiAl-14.5 Ta 4-point bend specimen produced by directional solidification.

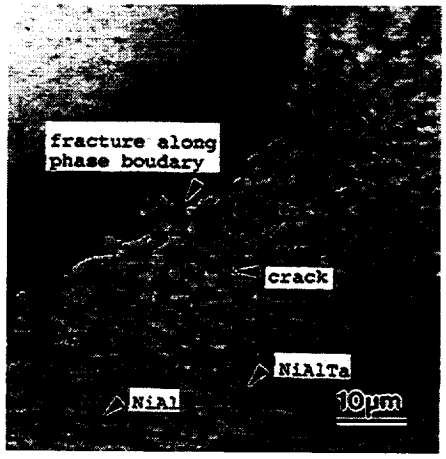

Figure 5: Light optical photomicrograph of the fracture region from a NiAl-14.5 Ta alloy.

POLYPHASE IN-SITU COMPOSITES

While the NiAl-refractory metal eutectics have lower creep strengths than the NiAl-Laves phase alloys, they have a much higher fracture toughness, such as the NiAl-Cr eutectic listed in Table 2. Thus, it may be possible to blend the high temperature properties of the NiAl-NiAlTa eutectic with those of the NiAl-refractory metal eutectics in a multiphase alloy provided that such systems thermodynamically exist.

Fortunately, a number of ternary eutectics have been located in the NiAl-NiAlTa-refractory metal systems [14] and these are listed in Table 3.

Table 3: Preliminary data for ternary eutectics consisting of NiAl, NiAlTa, and a refractory metal phase.

Composition (atomic %)	Volume fractions NiAl	NiAlTa	Metal	Melting temperature
Ni-42.05Al-12.5Ta-7Mo	58	18	24	1798 K
Ni-30.5Al-6Ta-33Cr	37	25	38	1710 K
Ni-28.5Al-10Ta-33V	26	29	45	1617 K

Representative microstructures of these eutectics are shown in Figure 6. Work is currently in progress to determine the mechanical properties from directionally solidified ingots of these compositions.

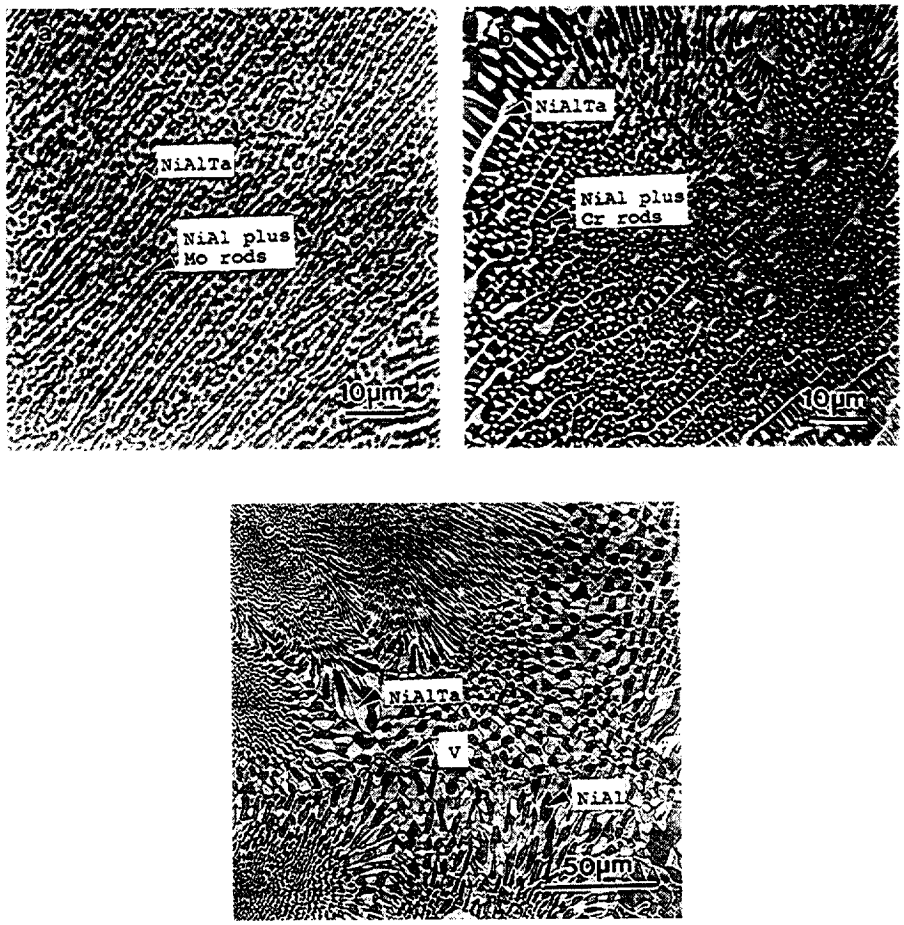

Figure 6: Light optical photomicrographs of ternary eutectics consisting of NiAl, NiAlTa, and a refractory metal.
(a) NiAl-NiAlTa-Mo
(b) NiAl-NiAlTa-Cr
(c) NiAl-NiAlTa-V

CONCLUSIONS

1. Promising creep strengths were measured from a directionally solidified NiAl-NiAlTa (NiAl-14.5 Ta) alloy.

2. The increase in creep strength of the NiAl-NiAlTa alloy over that of NiAl was not gained at the expense of room temperature fracture toughness.

3. Polyphase in-situ composites employing NiAl, NiAlTa, and a refractory metal are currently being examined to enhance the combination of room temperature toughness and elevated temperature creep strengths.

ACKNOWLEDGMENT

The authors wish to acknowledge financial support and cooperative research with NASA Lewis Materials Laboratory through grant NAG3-876. Appreciation is extended to Matt Ferber of the High Temperature Materials Laboratory at Oak Ridge National Laboratory for the use of the 4-point flexure fixture.

REFERENCES

1. R. Darolia, JOM, March (1991), 44-49.

2. G. Sauthoff, Z. Metallkde., 81 (1990), 855-861.

3. G. Sauthoff, Intermetallic Compounds - Structure and Mechanical Properties, O. Izumi, ed., The Japan Institute of Metals, Sendai, Japan, (1991), 371-378.

4. J. D. Whittenberger, R. Reviere, R. D. Noebe and B. F. Oliver, Scripta Met. Mater., 26 (1992), 987-992.

5. P. Nash and D. R. F. West, Met. Sci., 12(13) (1979), 670-676.

6. R. D. Reviere, B. F. Oliver, and D. D. Bruns, Mat. & Manufacturing Processes, 4(1) (1989), 103-131.

7. D. R. Johnson, S. M. Joslin, R. D. Reviere, B. F. Oliver, and R. D. Noebe, Processing and Fabrication of Advanced Materials for High Temperature Applications-II, V. A. Ravi and T. S. Srivatsan eds, TMS, Warrendale, PA (1993), 77-90.

8. W. F. Brown and J. E. Srawley, Plane Strain Crack Toughness Testing of High Strength Metallic Materials, ASTM Special Publication No. 410, ASTM, Philadelphia, PA, (1966), 13-14.

9. J. D. Whittenberger and R. D. Noebe, unpublished data, 1991.

10. D. R. Johnson, S. M. Joslin, B. F. Oliver, R. D. Noebe, and J. D. Whittenberger, Intermetallic Matrix Composites II, D. Miracle et al., eds., MRS Vol. 273, Pittsburgh PA, (1992), 77-90

11. M. V. Nathal and L. J. Ebert, Metall. Trans. A, 16A (1985), 1863.

12. K. S. Kumar, S. K. Mannan, and R. K. Viswanadham, Acta Metal. Mater., 40 (1992), 1201-1222

13. S. Reuss, and H. Vehoff, Scripta Met., 23 (1990), 1021-1026.

14. D. R. Johnson, Ph.D. thesis, University of Tennessee, (in progress).